Journal of Solid State Chemistry 184 (2011) 633–636

Contents lists available at ScienceDirect

Journal of Solid State Chemistry

journal homepage: www.elsevier.com/locate/jssc

Catalytic synthesis of bamboo-like multiwall BN nanotubes via SHS-annealing process

L.P. Zhang [a], Y.L. Gu [a,b,*], J.L. Wang [a], G.W. Zhao [a], Q.L. Qian [a], J. Li [a], X.Y. Pan [a], Z.H. Zhang [a,b]

[a] School of Material Science and Engineering, Wuhan Institute of Technology, Wuhan 430073, China
[b] Nano and Ceramic Materials Research Center, Wuhan Institute of Technology, Wuhan 430073, China

ARTICLE INFO

Article history:
Received 29 September 2010
Received in revised form
8 December 2010
Accepted 16 January 2011
Available online 25 January 2011

Keywords:
Boron nitride
Nanotubes
Synthesis
SHS
Bamboo-like
Growth mechanism

ABSTRACT

Bamboo-like multiwall boron nitride (BN) nanotubes were synthesized via annealing porous precursor prepared by self-propagation high temperature synthesis (SHS) method. The as-synthesized BN nanotubes were characterized by the field emission scanning electron microscopy (FE-SEM), transmission electron microscope (TEM), high-resolution TEM (HRTEM), X-ray diffraction (XRD), Raman and Fourier transform infrared (FTIR) spectroscopy. These nanotubes have uniform diameters of about 60 nm and an average length of about 10 μm. Four growth models, including tip, base, based tip and base–tip growth models, are proposed based on the catalytic vapor–liquid–solid (VLS) growth mechanism for explaining the formation of the as-synthesized bamboo-like BN nanotubes. Chemical reactions and annealing mechanism are also discussed.

1. Introduction

After the first successful synthesis of single-walled boron nitride (BN) nanotubes in 1995 [1], different types of BN nanotubes have received increasing attention due to their remarkable properties such as stable insulators, high thermal conductivity, superb oxidation resistance, a band gap about 5.5 eV, distinguishable chemical stability and outstanding mechanical strength [2]. All of these unique properties give BN nanotubes great potential applications in electronics, optoelectronics, energy storage and nanoelectromechanical systems [3]. In addition, the BN nanotubes were also predicted to be applicable in gas adsorbents, spintronic devices, UV lasers, high resistivity substrates, interconnects for nanoscale electronics, radiation stoppers and reinforcing agents for functional airspace metals/ceramics [4]. Until now, there have been many different synthetic techniques developed to grow BN nanotubes, including arc-discharge, laser ablation, ball-milling, plasma-jet, substitution reactions with carbon nanotubes as templates, and chemical vapor deposition (CVD) [5].

According to literature, the bamboo-like BN nanotubes have a higher gravimetric hydrogen uptake capacity [6]. On the other hand, they may exhibit more excellent elastic properties and mechanical stiffness due to their unique wall-structures compared to the other nano-structures of BN nanotubes. It has been reported that the bamboo-like BN nanotubes can be synthesized by heating B/Fe_2O_3 [7] or barium metaborate [8] in flowing ammonia gas. Bamboo-like BN nanotubes also can be fabricated by annealing ball-milled graphite/BN powders [9] and $B/B_2O_3/NH_3$ [10,11], amorphous boron/Eu/NH_3/N_2 [12]. In addition, the bamboo-like BN nanotubes were successfully prepared using CVD from B–N–O precursor/NH_3 [6], and Si/Al/Fe/B_2H_6/NH_3/O_2/Ar [3]. Although these methods can synthesize bamboo-like BN nanotubes, the yields and purity are disappointingly low.

In this communication, we report an effective CVD method by annealing porous precursor to synthesize bulk bamboo-like multiwall BN nanotubes. The porous precursor is prepared by self-propagation high temperature synthesis (SHS) method. Based on experimental results, four growth models of catalytic vapor–liquid–solid (VLS) growth mechanism are proposed. Chemical reactions and annealing mechanism are also discussed.

2. Experimental

The raw materials, 20.00 g CaB_6 and 20.00 g Fe_2O_3 (both above 300 mesh, 99.5 wt%) were mixed adequately by a blender for 30 min. The mixture was put into a SHS-furnace and heated to 750 °C for 10 min in an argon atmosphere under normal pressure. After combustion reaction, 38.47 g porous precursor was then obtained. The porous precursor was placed in an alumina boat and heated in the annealing furnace to 1150 °C at 6 °C/min keeping for 6 h in ammonia atmosphere at a flow rate of 0.8 L/min under

* Corresponding author. Fax: +86 27 8719 3199.
E-mail address: ncm@mail.wit.edu.cn (Y.L. Gu).

0022-4596/$ - see front matter © 2011 Elsevier Inc. All rights reserved.
doi:10.1016/j.jssc.2011.01.016

normal pressure. After the furnace cooled to room temperature, the crude product was collected, and then stirred in 400 mL HCl solution (15 wt%) at 80 °C for 24 h to remove byproducts and metal catalyst. The precipitates were filtered, washed by distilled water and dried in a vacuum oven at 80 °C for 12 h. Finally, 22.06 g gray product powders were obtained with a yield of about 81.4 wt% with respect to boron.

The structures of the sample were investigated by X-ray diffraction analysis (XRD) using a Shimadzu XD-5A diffractometer with Cu$K\alpha$ radiation (wavelength $\lambda=1.5406$ Å). The field emission scanning electron microscopy (FE-SEM) analysis was employed to examine sample morphology using a FEI Sirion 200 microscope. For FE-SEM observation, the samples were prepared by directly spreading the product powder on conductive tapes and spattering Au or Pt on the surface. The morphology and structure of the sample were further elucidated by transmission electron microscope (TEM) and high-resolution TEM (HRTEM) in a JEOL JEM-2100 microscope. For TEM and HRTEM observations, the samples were prepared by ultrasonically dispersing the product in ethanol, and depositing on copper grids coated with carbon film. Raman spectra were recorded at room temperature on a Nicolet DXR Raman spectrometer using Nd:YAG laser at excitation of 532 nm. Fourier transform infrared (FTIR) spectra were recorded on a Nicolet 6700 Fourier transform infrared spectrometer in transmission mode using a KBr wafer.

3. Results and discussion

Fig. 1 displays the typical FE-SEM, TEM and HRTEM images of the as-synthesized BN nanotubes. The typical FE-SEM image of the as-synthesized sample in Fig. 1(a) shows the general morphological characteristics. It presents a large quantity of one-dimensional (1D) nano-structures with uniform diameters of about 60 nm and an average length of about 10 μm. In addition, a small amount of BN flakes can be observed. Nanotube content is estimated as approximately 80 wt% according to the statistical analyses by TEM and FE-SEM microscopy. To confirm the detailed morphology and structure, a respective extensive TEM investigation was carried out. Fig. 1(d) reveals a representative TEM image of an individual BN nanotube consisting of a row of periodic cup-stack, bamboo-like structures. It also clearly displays that the tube has an outer diameter of about 60 nm and an inner diameter of 20 nm.

A corresponding HRTEM image (Fig. 1(b)) was recorded from a part of the BN nanotube. It is demonstrated that the lattice fringes are well-defined, suggesting that the nanotube wall has a high degree of crystalline perfection. Fig. 1(c) shows the magnified image of the BN nanotube (the frame in Fig. 1(c)). It clearly reveals lattice fringes having an interlay distance of 0.34 nm, which is close to the intershell spacings of the {002} lattice planes of the hexagonal phase of BN.

Fig. 2 shows the XRD pattern (a), Raman spectrum (b), wide-scan FTIR spectrum (c) and the deconvulation FTIR spectrum (d) of the as-synthesized BN nanotubes. The typical XRD pattern shown in Fig. 2(a) reveals five diffraction peaks at d-spacings of 3.394, 2.162, 2.067, 1.641 and 1.251 Å, that can be indexed as the (002), (100), (101), (004) and (100) planes of hexagonal phase of BN. The lattice constants are $a=2.516$ and $c=6.712$ Å, which is close to the value $a=2.503$ and $c=6.661$ Å in PCPDF card no. 73-2095. The fact that no other diffraction peaks are observed indicates that the as-synthesized product has high purity of BN without impurities such as CaB_6, Fe_2O_3 and other crystalline phases. The XRD analysis reveals that the as-grown product is pure hexagonal structure BN.

Fig. 2(b) is the typical Raman spectrum of the as-synthesized BN nanotubes, which shows a sharp peak at 1356 cm^{-1}, corresponding to the hexagonal BN active mode, E_{2g}, derived from the in-plane atomic displacement of the B and N atoms toward each other [6]. More information of the lattice vibrations can be gained through FTIR characterization. A typical FTIR spectrum presented in Fig. 2(c) shows strong vibrations at 793 and 1370 cm^{-1}, indexed to the A_{2u} (BN vibration out-of-plane polarization) and E_{1u} (BN vibration in-plane polarization) mode, respectively. The broad absorption band near 3401 cm^{-1} can be resulted from the O–H bonds due to the absorbed water. Two peaks at about 1210 and 1530 cm^{-1} emerge in the deconvulation spectrum (Fig. 2(d)) of the main peak around 1370 cm^{-1}. The former can be indexed to vibrations like those of wurtzite BN possibly for structure defects in the as-grown cylinder type of BN nanotubes. The later is due to the stretching of the hexagonal BN network along the tangential directions (T-mode), which is the characteristic absorption of well-crystallized BN nanotubes.

In the growth process of the bamboo-like BN nanotubes, the chemical reactions can be formulated as follows:

$$3CaB_6+2Fe_2O_3=B_{18}Fe_4Ca_3O_6 \quad (1)$$

$$B_{18}Fe_4Ca_3O_6+18NH_3=18B^*+18N^*+Fe_4Ca_3O_6+27H_2 \quad (2)$$

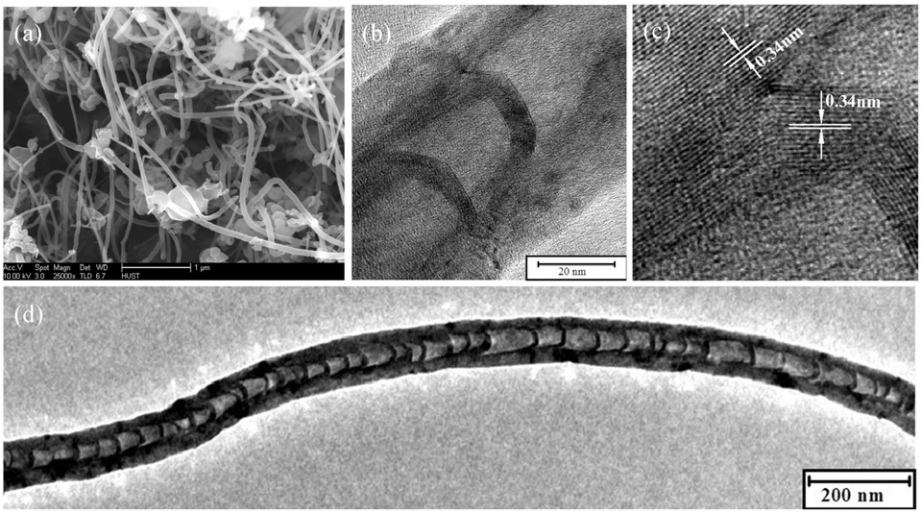

Fig. 1. FSEM (a), TEM (b) and HRTEM (c, d) images of the as-synthesized BN nanotubes.

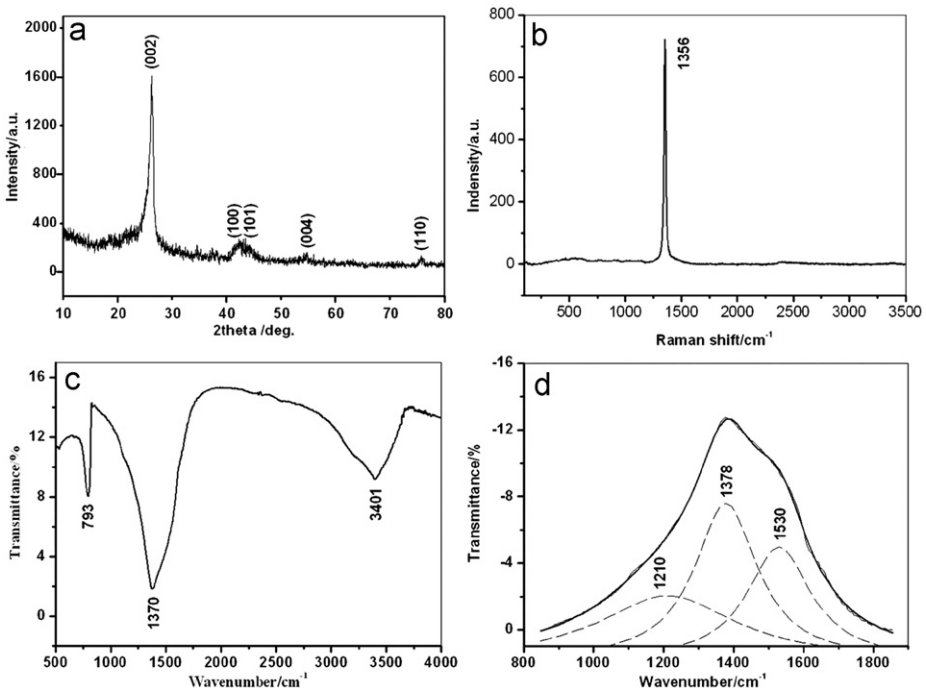

Fig. 2. XRD pattern (a), Raman spectrum (b), wide-scan FTIR spectrum (c) and the deconvulation FTIR spectrum (d) of the as-synthesized BN nanotubes.

$$x(B^*+N^*)+Fe_4Ca_3O_6 = xBN_{NT}+3FeO+3CaO+Fe \quad (3)$$

$$(18-x)(B^*+N^*)=(18-x)BN_{FL}$$
$$(x=0\text{–}18,\ NT=\text{nanotubes},\ FL=\text{flakes BN}) \quad (4)$$

As shown in Eq. (1), the porous precursor $B_{18}Fe_4Ca_3O_6$ is prepared by SHS method from the raw material CaB_6 and Fe_2O_3 powders. The SHS synthesis generally results in very high yields above 95 wt%, so the chemical composition formula of the precursor can be expressed approximately as $B_{18}Fe_4Ca_3O_6$. During the annealing process, boron-catalyst-containing species in the precursor reacts with NH_3 and produced active boron (B^*) and nitrogen (N^*) vapor (Eq. (2)). Liquid droplets of catalyst Fe or Fe–Ca alloy support on CaO particles, expressed as $Fe_4Ca_3O_6$ can be simultaneously generated in-situ from metal borides and oxides. According to the catalytic VLS growth mechanism [13], BN nanotubes can be grown from the B^* and N^* vapor in the presence of the catalyst (Eq. (3)). Small amount of BN flakes (as seen in Fig. 1(a)), may also be produced through a vapor–solid (VS) growth mechanism due to lacking of catalyst (Eq. (4)). Therefore, the selectivity of BN nanotubes can be expressed as $x/18$, where the value of x is estimated as approximately 14.5 according the selectivity of the as-synthesized BN nanotubes.

Fig. 3 is the schematic illustrations of the growth models of the as-synthesized bamboo-like BN nanotubes. It includes four growth models co-existing in the growth process, namely base, tip, based tip and base–tip growth models shown in Fig. 3(a)–(d), respectively.

According to the catalytic VLS growth mechanism [13], bamboo-like BN nanotubes can be grown depending on abruptly changing of growth rate of individual BN nanotubes. Firstly, reactive boron sources and catalyst particles are dispersed homogeneously in the porous precursors. Both supported and free catalyst droplets can be formed in-situ during the annealing process at 1150 °C (see Fig. 3(a1), (b1) and (c1)). Then NH_3 is decomposed to the active N^* and adsorbed on the surface of the catalyst particle. As mentioned in Eq. (2), active boron (B^*) and

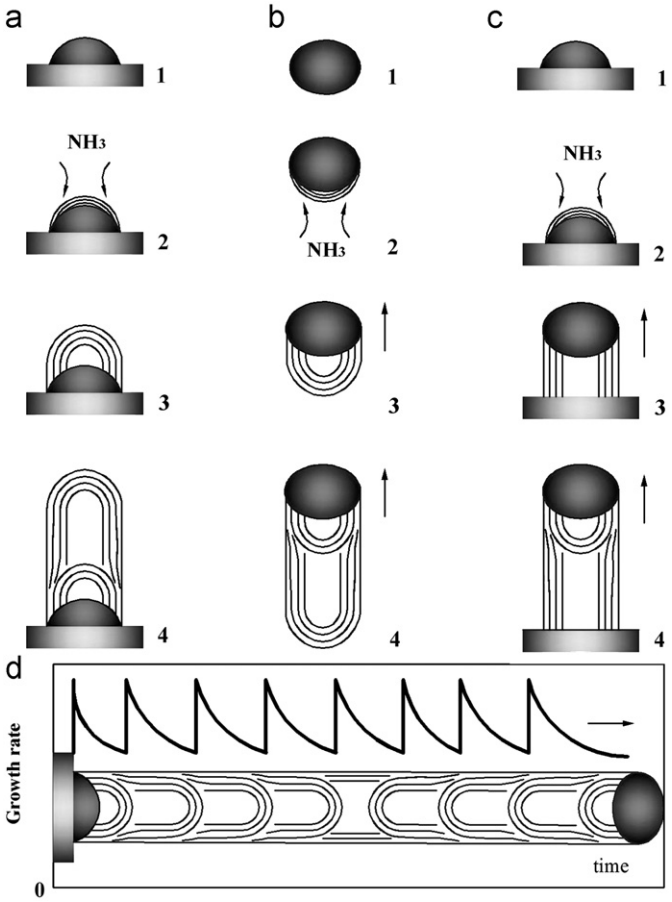

Fig. 3. Schematic illustrations of the as-synthesized BN nanotubes through (a) base growth, (b) tip growth, (c) based tip growth, (d) base–tip growth and corresponding features of growth rates. Black particles contain boron source and catalyst. The arrows denote the movement direction of the tip catalyst droplets.

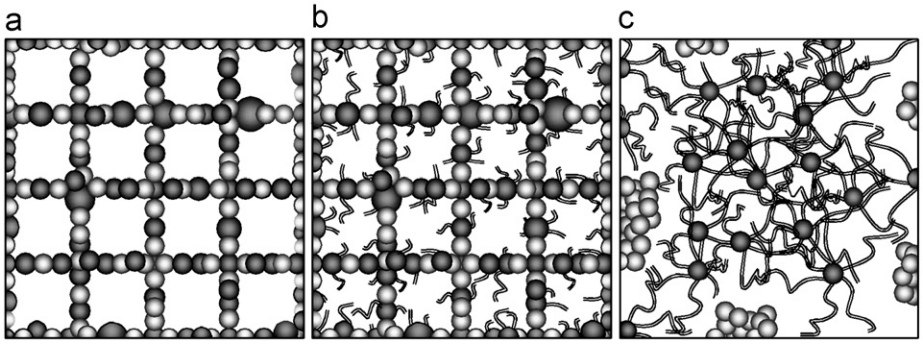

Fig. 4. Sketch of bulk synthesis of BN nanotubes by annealing porous precursor: (a) original state of porous precursors prepared by SHS, (b) catalytic sites and the initial growth stage of BN nanotubes, and (c) the final stage of fully annealed precursor. Black particles contain boron source and catalyst, while the gray denote catalyst support. The wool-like structures represent BN nanotubes.

nitrogen (N*) vapor form BN. The newly formed BN species precipitate layer by layer to form BN shells, as described in Figs. 3(a2), (b2) and (c2). The BN layers grow from the interface between the catalyst and BN shells (see Fig. 3(a3), (b3) and (c3)). With the gradual growth of BN nanotube, negative pressure of inner void is formed and liquid catalyst droplets are reshaped. While the pulling force generated by the negative pressure is too big to withstand, an instant disjoint occurs at the interface. At that moment, outside vapor containing B* and N* fly inside to balance the pressure, leaving an achieved bamboo knot structure (see Figs. 3(a4), (b4) and (c4)). And finally, the bamboo-like tube can grow up through repeating the process. Similar to the other three growth models described above, the bamboo-like BN nanotubes can also grow with base–tip growth mechanism (Fig. 3(d)). In fact, it has two growth points combining the base and tip growth mechanism. The characteristic growth rates for the bamboo-like BN nanotubes can be expressed as a periodic changing of growth rate, as shown in Fig. 3(d).

Fig. 4 is a sketch of bulk synthesis of BN nanotubes by annealing porous precursor. The structure of the porous precursor consists of boron source and catalyst sources (black particles) and inert support particles (gray, Fig. 4(a)). In the initial annealing stage, the BN nanotubes begin to grow mainly by base, based tip and base–tip growth models from boron source and catalyst particles (Fig. 4(b)). Importantly, the porous structure is kept well-structured during the quick and random growth of BN nanotubes. Bulk synthesis of BN nanotubes can be easily reached via unique SHS-annealing method accordingly. When the precursor is completely reacted, BN nanotubes push away and separate from the support particles, resulting in local agglomerates of wool-like BN nanotubes (Fig. 4(c)). Therefore, the porous structure of the solid precursor plays a key role in bulk synthesis of the as-grown BN nanotubes process.

4. Conclusions

In conclusion, bamboo-like multiwall BN nanotubes were successfully synthesized by a CVD method via annealing at 1150 °C in a flowing ammonia atmosphere using porous precursor prepared by SHS method. The as-synthesized bamboo-like BN nanotubes have uniform diameters of about 60 nm and a length of about 10 μm in average. Four growth models based on the catalytic VLS growth mechanism are proposed, so-called base, tip, based tip and base–tip growth models. Chemical reactions and annealing mechanism demonstrate that the porous precursor plays a crucial role in bulk synthesis of the as-synthesized bamboo-like BN nanotubes.

Acknowledgments

The authors acknowledge the financial support from the Government of Hubei Province of the People's Republic of China for this research work. The authors acknowledge Prof. Xu Liqiang (School of Chemistry and Chemical Engineering, Shandong University) for their help in assisting microscopy analyses.

References

[1] N.G. Chopra, R.J. Luyken, K. Cherrey, V.H. Crespi, M.L. Cohen, S.G. Louie, A. Zettl, Science 269 (1995) 966–967.
[2] G.Y. Guo, J.C. Lin, Phys. Rev. B 71 (2005) 165402.
[3] C.Y. Su, Z.Y. Juang, K.F. Chen, B.M. Cheng, F.R. Chen, K.C. Leou, C.H. Tsai, J. Phys. Chem. C 113 (2009) 14681–14688.
[4] D. Golberg, Y. Bando, C.C. Tang, C.Y. Zhi, Adv. Mater. 19 (2007) 2413–2432.
[5] D. Golberg, Y. Bando, Y. Huang, T. Terao, M. Mitome, C.C. Tang, C.Y. Zhi, ACS Nano. 4 (2010) 2979–2993.
[6] R. Ma, Y. Bando, H. Zhu, T. Sato, C. Xu, D. Wu, J. Am. Chem. Soc. 124 (2002) 7672–7673.
[7] C.C. Tang, M. Lamy de la Chapelle, P. Li, Y.M. Liu, H.Y. Dang, S.S. Fan, Chem. Phys. Lett. 342 (2001) 492–496.
[8] C.C. Tang, Y. Bando, C.H. Liu, S.S. Fan, J. Zhang, X.X. Ding, D. Golberg, J. Phys. Chem. B 110 (2006) 10354–10357.
[9] L.T. Chaddertona, Y. Chen, J. Cryst. Growth 240 (2002) 164–169.
[10] F.Q. Ji, C.B. Cao, H. Xu, Z.G. Yang, Chin. J. Chem. Eng. 14 (2006) 389–393.
[11] H.C. Choi, S.Y. Bae, W.S. Jang, J. Park, H.J. Song, H.J. Shin, J. Phys. Chem. B 109 (2005) 7007–7011.
[12] H. Chen, Y. Chen, B.C.P. Li, H.Z. Zhang, J.S. Williams, Y. Liu, Z.W. Liu, S.P. Ringer, Adv. Mater. 19 (2007) 1845–1848.
[13] R.S. Wagner, W.C. Ellis, Appl. Phys. Lett. 4 (1964) 89–90.